RSC Advances

PAPER

View Article Online
View Journal | View Issue

Check for updates

Cite this: *RSC Adv.*, 2021, **11**, 26284

Evaporation behavior of 2LiF–BeF_2–ZrF_4 molten salt with irradiated nuclear fuel

Jinhao Zhou,[ab] Junxia Geng,[abc] Yan Luo,[abc] Rongrong Cui,[ab] Zhongqi Zhao,[abc] Haiying Fu,*[abc] Qiang Dou,*[abc] Xiaohe Wang,[ab] Wenxin Li,[ab] Jingen Chen[abc] and Qingnuan Li[abc]

The evaporation behaviours of various components were investigated by using a low pressure distillation method in a 2LiF–BeF_2–ZrF_4 mixture containing irradiated ThF_4 and UF_4. The experiment showed that BeF_2 and ZrF_4 were found to mainly condensate at the outer cover, the coolest zone, and their relative volatilities *vs.* LiF were 9.8 and 32.2, respectively, while for ThF_4 and UF_4, at four different temperature zones the values were almost constant, at 0.1 and 0.3. The radioactivity of various nuclides was further detected using gamma spectrometer analysis. ^{137}Cs was hardly observed due to long half-time decay. ^{233}Pa was found to co-evaporate with the carrier salt, while ^{239}Np mainly remained in the residual salt as ^{237}U. In different temperature zones, the decontamination factors of rare earth in receiver salts ranged from 10 to 10^3. On the basis of the investigation, it was proposed that the distribution of various nuclides after distillation, may be helpful to design the feasible condensate system to recover the carried salt in a molten salt reactor.

Received 6th July 2021
Accepted 24th July 2021

DOI: 10.1039/d1ra05195d

rsc.li/rsc-advances

Open Access Article. Published on 01 August 2021. Downloaded on 5/2/2026 3:38:09 AM.
This article is licensed under a Creative Commons Attribution-NonCommercial 3.0 Unported Licence.

Introduction

A molten salt reactor (MSR) is usually considered to be a chemical reactor in which molten halides are used as the carrier of nuclear fuel and coolant. To improve neutron utilization, fission products with high neutron absorption cross sections should be separated on time. Pyrochemical reprocessing technology has proven to be the optimum method for treating MSR nuclear fuel.[1,2] In the 1960s, Oak Ridge National Laboratory (ORNL) projected a close-coupled processing facility for removing fission products and fissile materials from fused molten salt mixtures to be an integral part of a reactor system during molten salt breed reactor MSBR conceptual design.[3] In the last ten years, Shanghai Institute of Applied Physics (SINAP) has undertaken a thorium-based molten salt reactor (TMSR) programme, and developed the pyro-processing methods to separate uranium and recover the carrier salt from spent nuclear fuel, mainly based on the fluoride volatility method (FVM), low-pressure distillation and high-temperature electrochemistry.[4–10] Briefly, the discharged fuel salt was first reacted with fluorine, which would result in removal of uranium as a volatile UF_6. The salt would then be fed to a low-pressure (approximately 1 Torr) single-stage still where the ^7LiF and BeF_2 would be vaporized and recovered. Less volatile fluoride fission products would remain in a liquid heel in the still for further treatment. The recovered uranium and carrier salt would be reused.

In our integrated evaporation and condensing unit,[11] the technique of low-pressure distillation of molten salt has recently been demonstrated by using a simulated fluoride system for samples with weights ranging from grams to kilograms. Wang *et al.*[6] observed the evaporation behaviours of rare earth-doped FLiNaK melts during low-pressure distillation. The decontamination factors (DFs) of typical rare earth elements were deduced to be approximately 10^3, except for europium, which formed the volatile compound EuF_2. Y. Luo *et al.*[8] further investigated the effect of ThF_4 on the distillation of FLiNaK molten salt and explored possibilities for the recovery of carrier salts. Our results were consistent with those literatures.[12,13]

It is convenient to investigate the components by elemental analysis in a nonirradiated fuel salt system. However, studies of many fission products are not feasible because the variety of simulated additives is limited. For example, nuclide ^{233}Pa is the intermediate product formed by irradiated ^{232}Th, as shown in eqn (1); ^{233}Pa can then further convert into fissile nuclide ^{233}U after beta decay. ^{232}Th is internationally recognized as a potential nuclear resource. In SINAP, the target for TMSR program is to utilize thorium resources and achieve the thorium–uranium nuclear fuel cycle because the Th–U cycle shows a number of advantages, such as higher conversion to fissile nuclide in thermal reactors, much less minor actinides formed than in the U–Pu fuel cycle, and intrinsic proliferation resistance.

[a]*Shanghai Institute of Applied Physics, Chinese Academy of Sciences, Shanghai 201800, China. E-mail: fuhaiying@sinap.ac.cn; douqiang@sinap.ac.cn*

[b]*CAS Innovative Academies in TMSR Energy System, Chinese Academy of Sciences, Shanghai, Chinese Academy of Sciences, Shanghai 201800, China*

[c]*University of Chinese Academy of Sciences, Beijing 100049, China*

© 2021 The Author(s). Published by the Royal Society of Chemistry

Open Access Article. Published on 01 August 2021. Downloaded on 5/2/2026 3:38:09 AM.
This article is licensed under a Creative Commons Attribution-NonCommercial 3.0 Unported Licence.

$$^{232}_{90}\mathrm{Th} \xrightarrow{\beta} {}^{233}_{91}\mathrm{Pa} \xrightarrow{\beta} {}^{233}_{92}\mathrm{U} \quad (1)$$

To maintain the high efficiency of reactor operations and ensure the effective proliferation of ^{232}Th, ^{233}Pa and rare earth fission products must be separated from fuel in time. In ORNL, the metal reduction extraction technology developed to separate ^{233}Pa and rare earth fission products required high purity metal ^{7}Li (>99.95%) as a reducing agent.[14] However, ^{7}Li isotopes are very expensive, and the separation efficiency of reduction extraction was a little low. The evaporation behaviour was enhanced by using the distillation method. Although in ORNL, the engineering-level radioactive distillation experiments were carried out to determine the relative volatility of some fission nuclides, the irradiated mixture salt did not contain ThF_4, and ^{233}Pa was not observed.[15]

The purpose of this study was to demonstrate and characterize the evaporation behavior of various fluorides in mixture molten salt during low-pressure distillation. The 2LiF–BeF_2–ZrF_4 (expressed as FLiBe–ZrF_4) molten salt with irradiated ThF_4 and UF_4 fuels was first treated by fluorination process, where UF_4 was reacted with F_2 and the product, UF_6, was adsorbed by the adsorbant NaF at 823 K as our previous work.[4] Then the mixture salt was transferred to the low-pressure distillation equipment and the evaporation experiment was carried out at 1223 K and 30 Pa. The specific activity of radioactive nuclides was measured by a high-purity germanium detector HPGe gamma spectrometer. The behaviours of rare earth and noble metal fission products and actinide nuclides (^{233}Pa and ^{239}Np) were evaluated from the differences in specific activities of radioactive nuclides before and after distillation.

Experimental

Reagents and materials

LiF, BeF_2 and ZrF_4 with 99.99% purity were purchased from Sigma-Aldrich, China. ThF_4 with 99.9% purity was provided by the Changchun Institute of Applied Chemistry, Chinese Academy of Sciences, and the oxygen content was 4000 ppm. UF_4 (99.9%) was provided by China North Nuclear Fuel Co., Ltd. Ar gas with 99.999% purity was purchased from Shanghai Louyang Gas Co. Ltd. All other reagents were of analytical grade and were used without further purification.

2LiF–BeF_2–ZrF_4 salt (LiF–BeF_2–ZrF_4: 65–30–5 mol%) was prepared according to the procedures described in our previous work.[4] Certain amounts of fluorides (UF_4, ThF_4) and FLiBe–ZrF_4 with a mass ratio of 2 : 2 : 26 were mixed in a nickel crucible (Ni purity > 99.96%, Sinopharm Chemical Reagent Co., Ltd.), which was placed inside the furnace vessel. After the vessel was sealed by covering the lid and screwing tight, it was first heated to 523 K and maintained for 2 h to remove trace moisture. Then, the furnace was heated up to 973 K and kept at that temperature for 24 h. The prepared molten salt was naturally cooled.

Equipment

The experimental equipment for a low-pressure distillation was composed of a two-stage pit-type electric resistance furnace, an evaporator crucible, condensation sheets, a collected crucible, and a vacuum system, as shown in Fig. 1. The nickel crucible with inner diameter of 100 mm and height of 50 mm was used as the evaporator crucible. The collected crucible was welded with the integrated sleeve. And the outer condensation sheet was designed to tightly cover the integrated sleeve, which provided a closed chamber to minimize the loss of salt. The distillation experiment was conducted in a glove box with an argon atmosphere (99.999%), and the oxygen and water contents in the glove box were both below 1 ppm.

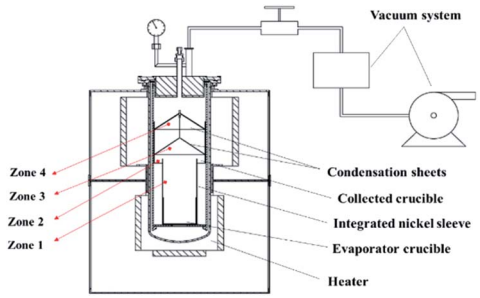

Fig. 1 Schematic of the experimental apparatus for low pressure distillation.

It is known that the bottom heater works, the temperature distribution of the chamber was not equal. When the temperature reaches 1223 K, we divided four different temperature zones, and the centre temperatures in the four zones from No. 1 to No. 4 were determined using process temperature control blocks (JFCC, Japan). The process was as following: after four blocks were fixed on the surface, the empty chamber was heating to 1223 K and kept 4 h, and the pressure was 30 Pa. Then the chamber was generally cooling to room temperature. According to the size of each block, the temperature was confirmed to 1123 K, 1053 K, 923 K and 773 K from zone 1 to zone 4, respectively. During the distillation experiment, the temperature and pressure data were automatically monitored and recorded by the control software.

Experimental method

UF_4 and ThF_4 targets, loaded separately in sealed acrylic (polymethyl methacrylate) boxes, were irradiated using a photoneutron source (PNS) at the Shanghai Institute of Applied Physics, CAS, China. The PNS was derived from a 15 MeV electronic accelerator. The maximum neutron yields reached around 1.2×10^{11} s^{-1}, total fluence being about 3×10^{13} n and the average energy of the neutrons was approximately 1 MeV.[16] After irradiation for 3 days and cooling for 24 h, the salt mixture was prepared.

The FLiBe–ZrF_4–ThF_4–UF_4 samples were loaded into a nickel crucible after fluorination treatment and then placed in the heating zone of the still. The evaporating zones were heated to 823 K with a heating rate of 10 K min^{-1}, and the condensing zone was not heated. The temperature was maintained at 823 K for 60 min until the salt melted completely, after which it was eventually raised to 1223 K with 10 K min^{-1}. The distillation

Open Access Article. Published on 01 August 2021. Downloaded on 5/2/2026 3:38:09 AM.
This article is licensed under a Creative Commons Attribution-NonCommercial 3.0 Unported Licence.

chamber was kept around 1000 Pa before 1223 K to prevent the evaporation during heating. When the temperature reached the given temperature, the inner pressure of the salt distiller was reduced by a vacuum pump. The pump kept running until the experiment was over and the pressure inside the evaporator was about 30 Pa. Salt vapor was condensed and deposited onto the different surfaces and the sample salts were collected individually from zone 1 to zone 4 as Fig. 1.

In addition, to observe more nuclides, the fluorination process was intentionally left incomplete at 823 K, 4 h, and about 20 wt% UF_4 remained in the mixture salt.

Measurement and data analysis

The contents of elements in the crude salt, residual salt and condensate salts of different zones were analysed by inductively coupled plasma-mass spectroscopy (ICP-MS, Optima 8000, PE Company).

Φ was used to evaluate the evaporation ratio of the total mass of condensate salts (w_1), which was obtained from zone 1 to zone 4 and the crude salt weight (w_0) as in eqn (2):

$$\Phi = \frac{w_1}{w_0} \times 100\% \quad (2)$$

The effective relative volatility of a component with respect to LiF, α_{i-LiF}, is defined as in eqn (3):[6–9]

$$\alpha_{i-LiF} = \frac{y_i/x_i}{y_{LiF}/x_{LiF}} \quad (3)$$

where y is the mole fraction in the condensates and x is the mole fraction in the evaporator pot.

The specific activity for the radionuclides were measured by a high-purity germanium detector (HPGe) at room temperature. The HPGe detector (model GEM30P4-76-PL) was supplied by ORTEC, USA. The energy resolution for a 1.33 MeV γ-ray is 1.85 keV, and the efficiency *versus* energy curve for the HPGe γ-ray detector at the counting distances was determined using a set of standard γ-ray point sources (^{152}Eu, ^{60}Co and ^{137}Cs). The counting times varied from 1 to 24 h, depending on the activities of the nuclides of interest.[17–19] The detector was cooled using liquid nitrogen to minimize dark current. The uncertainties in activities determined experimentally in this work are standard deviations, which are mainly derived from the statistical errors in the γ-ray counts, a 5–6% error in detector efficiency, and a 5% error in sample geometry. In general, the uncertainties in this work for given nuclides were approximately 20% or less.

To determine the change in the specific activity of radioactive nuclides during low-pressure distillation, the crude salt, residual salt and receiver salts were analysed. Approximately 0.3 g salt samples were crushed and meshed completely and then packed in quartz tubes (diameter 3 mm) for gamma spectrometry measurements.

Decontamination factors (DF) are an important parameter for evaluating the separation efficiency. Higher DF values indicate better separation efficiency. In this work, DF was deduced as eqn (4):

$$DF = \frac{A_0 \times M_0}{A_1 \times M_1} \quad (4)$$

where A_0 is the specific activity of the fission product before distillation, in units of Bq g^{-1} salt; M_0 is the total mass of the salt mixture before distillation, in g. A_1 is the specific activity of the fission product in receiver salt after distillation, in Bq g^{-1} salt. M_1 is the mass of salt received after distillation, in g.

Results and discussions

Mass balance of major components

After the fluorination process, approximately 160.0 g salt with irradiated UF_4 and ThF_4 was used in the distillation experiment. The mass of crude salt, residual salt and receiver salt distributed in four zones was measured by electronic balance, as shown in Table 1. The structure of each sample was determined by X-ray diffraction analysis at room temperature. Some complex was recognized as Li_2BeF_4, Li_2ZrF_6 in crude salt, and Li_3ThF_7, Li_2UF_6 in residual salt. The phenomena were similar as room temperature ionic liquid, which showed the intermolecular interaction.[20]

When the distillation experiment was carried out at approximately 30 Pa and 1223 K for 4 h, approximately 138.0 g of salt was evaporated, and 137.7 g of salt was collected in four zones. The evaporation ratio Φ was 86%, and the average distillation rate was 6.7 mg cm^{-2} min^{-1}. The total collection ratio was approximately 99%, and the condensate salts were clean and white, while the residual salt left in the nickel crucible was green, which may have resulted from the residual species UF_4.

The concentrations of various fluoride salts were measured by ICP-MS, as shown in Table 2. The mole fraction of UF_4 in crude salt was 0.68%. The salt showed light yellow colour. The mole fraction of UF_4 in residual salt increased to 4.48% and the colour of salt became green. The effective relative volatilities of the components collected in different zones with respect to that of LiF were further calculated. The data showed that ZrF_4 and BeF_2 evaporated easily, which was consistent with the vapor pressure of each single species.[21] The volatilities of UF_4 and ThF_4 were lower than that of LiF. For ZrF_4 and BeF_2, the relative volatility in low temperature zone was greater than that of high temperature zone, which indicated that BeF_2 and ZrF_4 should be condensated and collected in lower temperature zone. These values were in reasonable agreement with data from the reports from ORNL, in which the relative volatilities were calculated to be between 1173 K and 1323 K.[13,22]

Evaporation behavior of various nuclides

Various chemical species were produced after ThF_4 and UF_4 irradiation, including noble gases, noble metals, rare earth

Table 1 The mass of salt in different zones

	Crude salt	Residual salt	Receiver salt			
			Zone 1	Zone 2	Zone 3	Zone 4
The mass (g)	160.0	22.0	60.0	31.0	18.7	28.0

© 2021 The Author(s). Published by the Royal Society of Chemistry

Open Access Article. Published on 01 August 2021. Downloaded on 5/2/2026 3:38:09 AM.
This article is licensed under a Creative Commons Attribution-NonCommercial 3.0 Unported Licence.

Table 2 Major component of mixture salt by ICP-MS

		Mole fraction%					α_{i-LiF}			
		LiF	BeF_2	ZrF_4	ThF_4	UF_4	BeF_2	ZrF_4	ThF_4	UF_4
Crude salt		64.6	30.1	4.19	0.44	0.68	—	—	—	—
Residual salt		89.96	1.06	0.24	3.64	4.48	—	—	—	—
Receiver salt	Zone 1	80.24	18.27	1.19	0.072	0.28	0.49	0.23	0.13	0.33
	Zone 2	59.4	38.95	1.43	0.041	0.19	1.41	0.371	0.10	0.304
	Zone 3	21.6	70.2	7.66	0.074	0.18	6.98	5.47	0.05	0.79
	Zone 4	13.08	59.56	27.28	0.011	0.0066	9.78	32.16	0.12	0.048

metals, alkaline earth metals and actinide elements. Fig. 2 shows the γ-ray energy spectrum of fluorinated FLiBe–ZrF_4 containing UF_4 and ThF_4 irradiated at 823 K, *i.e.*, the crude salt before distillation. Kr and Xe were not detected because of gas state and alkali metal nuclide ^{137}Cs was not observed, either, due to its long half-time decay, and other nuclides were observed successfully. The total radio-activities of, for example, noble metal products ^{99}Mo, ^{103}Ru, and ^{95}Nb, halide ^{131}I, alkali earth metal ^{140}Ba, rare earth fission products ^{141}Ce, ^{143}Ce, ^{140}La and ^{147}Nd, and heavy elements ^{239}Np, ^{233}Pa, and ^{237}U, were calculated by the specific activity and the mass of condensation salt as Table 3.

After distillation, the specific activities of nuclides in residual and receiver salt were also deduced by energy spectrum detection. The results showed that the radioactivity of ^{131}I, ^{99}Mo, ^{95}Nb and ^{103}Ru in different samples were very low. Specifically, the contents in the residual salt were below the detection limit of the instrument.

Noble metal fission products

Before distillation, the FLiBe–ZrF_4 mixture salt containing irradiated ThF_4 and UF_4 was treated using F_2 bubbling at 823 K. As is known, F_2 can oxidize many low valence species, such as UF_4, iodide, molybdenum and ruthenium, and the products was UF_6, IF_5, MoF_6 or RuF_5, and so on, which all have high vapor pressure and low boiling points. These products were volatile and fixed to the adsorption column during the fluorination process. Therefore, the radioactivity of ^{131}I, ^{99}Mo, and ^{103}Ru in crude salt before distillation were low. And after distillation at high temperature 1223 K and low pressure of 30 Pa, such nuclides remaining in the mixture salt was evaporated again and condensated in the lowest temperature zone 4 or flowed into the off-gas.

^{95}Zr and ^{95}Nb was special nuclides. The high activity of ^{95}Zr in the receiver salt indicated its high volatility. As a daughter of the ^{95}Zr parent, the ^{95}Nb in the ^{95}Zr–^{95}Nb growth–decay mode showed activity that increased continually from almost zero to a maximum value. Under the experimental conditions, ^{95}Nb activity was not easily measured because the detection time was shorter than its half-life, which is 67 days. Therefore, the amount ^{95}Nb would be predicted to grow with the decay of ^{95}Zr in the receiver salt.

The radioactivity of ^{95}Nb in the FLiBe salt was found to change according to the redox potential of the molten salt.[23] Under oxidizing conditions, niobium mainly existed in the salt, but niobium was deposited on the alloy under reducing conditions. Therefore, NbF_5 may be generated when UF_4 reacts with fluorine gas at 823 K in FLiBe molten salt, and NbF_5 entered the adsorption column due to its volatility. Hence, noble metal fission nuclides were hardly observed in the crude salt before distillation.

Alkali earth and rare earth fission products

Alkali earth metal showed the similar properties as rare earth fission products, which are stable in mixture salt during fluorination process. The radioactivity of ^{140}Ba ^{141}Ce, ^{143}Ce, ^{140}La and ^{147}Nd was measured according the energy spectra, listed in Table 3, while some stable nuclides with large neutron cross-sections, such as ^{151}Sm and ^{149}Sm, were not detected. However, it is difficult to apply chemical analysis methods to examine the concentrations, because the neutron flow was very low and the

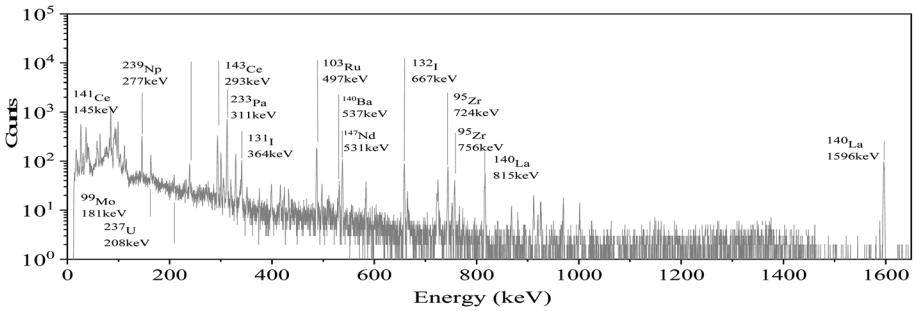

Fig. 2 γ-Ray energy spectrum of FLiBe–ZrF_4 salt containing irradiated UF_4 and ThF_4 before distillation.

Open Access Article. Published on 01 August 2021. Downloaded on 5/2/2026 3:38:09 AM.
This article is licensed under a Creative Commons Attribution-NonCommercial 3.0 Unported Licence.

Table 3 The radioactivities of different nuclides[a]

		Radioactivity (Bq)					
				Receiver salt			
Nuclide	$T_{1/2}$/day	Crude salt	Residual salt	Zone 1	Zone 2	Zone 3	Zone 4
^{140}Ba	12.75	39 440	35 057	990	182.9	1127.6	180
^{141}Ce	32.5	14 539	10 236	141	ND	439.5	ND
^{143}Ce	1.377	19 488	16 417	300	89.9	495.55	ND
^{140}La	1.679	36 840	30 564.6	759	126	1051	13.44
^{147}Nd	11	8667.2	8630.6	ND	ND	353.62	144.2
^{131}I	8.021	ND	ND	ND	7.75	46.75	ND
^{99}Mo	2.747	16 528	2752.2	366	ND	332.5	ND
^{103}Ru	39.26	2860.8	998.8	ND	ND	105	ND
^{95}Zr	64.03	10 355	ND	1830	ND	318.8	3088.44
^{95}Nb	34.99	ND	ND	301.2	ND	31 416	175.92
^{239}Np	2.356	5.03×10^5	3.44×10^5	8.84×10^4	1.13×10^4	1.63×10^4	1.46×10^2
^{233}Pa	26.98	1.10×10^5	1210	2.18×10^4	3.41×10^4	2.00×10^4	9.11×10^3
^{237}U	6.75	1.29×10^6	8.86×10^5	2.50×10^5	3.80×10^4	4.71×10^4	3.55×10^2

[a] Note: ND means no detected.

mass of fission nuclides was around 10^{-13} g. We evaluated the decontamination factors in four zones by eqn (4) as Table 4.

The decontamination factors of receiver salts in different zones were range from 20 to 3000. In our previous work, we measured the separation degrees of rare earth fluorides in a simulated FLiNaK melt.[6] The decontamination factor (DF) was almost 1000 at 1173 K. There are several main reasons for the low decontamination factors in this work. Firstly, the distillation temperature and content of fission products may affect the separation efficiency. The higher temperature may improve the evaporation rate and liquid entrainment occurred, which led to decrease DF value. Secondly, in the simulation experiment, the content of each rare earth fluorides was approximately 3 wt%, and chemical analysis was feasible to measure the component. While in this work, the absolute mass for each nuclide was less than 10^{-13} g after neutron radiation. The specific activity of rare earth fission in the crude salt was less than 1000 Bq g^{-1} salt and almost 0.5–4 Bq g^{-1} salt in condensate salt from zone 4. The very low content caused measurement certain inaccuracy up to 20%. Lastly, in the later stage of the distillation process, the content of fission products increased in crude salt, and some species may have co-evaporated with the carrier salt, which caused higher volatility of fission products.

On the other hand, the large difference of decontamination factors in different zones may be due to the cross-influence of condensed salts. For example, the temperature of zone 3 was more than 900 K, some of the condensed salt in zone 3 could flow back to zone 2 during distillation. Under our experimental conditions, it was not convenient to collect all the condensing salts in the best temperature zone. This needs to be improved in the future process devices.

Table 4 Decontamination factors (DF) of fission products

	Decontamination factor			
Nuclide	Zone 1	Zone 2	Zone 3	Zone 4
^{140}Ba	39.8	215.6	35	219.1
^{141}Ce	103.1	—	33	—
^{143}Ce	65	216.8	39.3	—
^{140}La	48.5	295	35	2741
^{147}Nd	—	—	24.5	60.1

Actinide nuclide

The evaporation behavior of actinide nuclides, such as ^{233}Pa, ^{239}Np and ^{237}U, were also observed.^{233}Pa is the intermediate nuclide in the ^{232}Th–^{233}U conversion chain as eqn (1), which has a relatively high thermal neutron capture cross section, and its half-life is 26.98 days. The conversion rate of thorium and uranium is directly reduced by consuming the precursor nucleus of the fission-prone nucleus. On the other hand, the reactor reactivity is reduced due to the consumption of neutrons, and the production of ^{233}U is indirectly affected.

To maintain the high efficiency of reactor operations and ensure the effective proliferation of ^{232}Th, ^{233}Pa and rare earth fission products should be separated from fuel in time. In ORNL, the metal reduction extraction technology developed to separate ^{233}Pa and rare earth fission products required high purity metal ^{7}Li (>99.95%) as a reducing agent.[14] However, ^{7}Li isotopes are very expensive, and the separation efficiency of reduction extraction is low. The evaporation behavior was enhanced by using the distillation method. Although ORNL carried out engineering-level radioactive distillation experiments to determine the relative volatility of rare earth fission nuclides, the molten distilled salt did not contain irradiated ThF_4, and ^{233}Pa was not further observed.[15] In the present work, the radioactivity change of ^{233}Pa was obvious as Table 3. In the crude salt before distillation ^{233}Pa was detected to1.1×10^5 Bq and the radioactivity was 1210 Bq in the residual salt after distillation which meant ^{233}Pa was co-evaporated with carrier salt and was more volatile than rare earth fission nuclides. The distribution of ^{233}Pa in condensate salts was 2.18×10^4, $3.41 \times$

© 2021 The Author(s). Published by the Royal Society of Chemistry

Open Access Article. Published on 01 August 2021. Downloaded on 5/2/2026 3:38:09 AM.
This article is licensed under a Creative Commons Attribution-NonCommercial 3.0 Unported Licence.

10^4, 2.00×10^4, 9.11×10^3 Bq, respectively. The lowest temperature zone 4, only 10% ^{233}Pa was founded and more than 90% ^{233}Pa was observed at the higher condensate temperature zones. On the other hand, the total activity from zone 1 to zone 4 was 8.5×10^4 Bq. This showed the total balance ^{233}Pa was not good. The similar phenomena were also observed by Zhao *et al.*[17] They found the reduction–deposition phenomena for ^{233}Pa in the FLiBe–ThF_4 mixture salt. Small amount of ^{233}Pa was found to deposit on the surfaces of the graphite crucible, but after adding Hastelloy C276 or metallic lithium, large number of ^{233}Pa was observed to deposit on the surface of the Hastelloy C276 and the bottom of the FLiBe salt. The redox character of a molten salt proved to affect the behaviour of protactinium in the salt system. In the distillation experiment under vacuum environment, we assumed that the nickel crucible may reduce ^{233}Pa and some Pa deposited on the surface of metal still, which resulted in the loss of protactinium.

Another actinide nuclide ^{239}Np was formed from a (p, n) reaction of ^{238}U, as shown in eqn (5) and ^{237}U was detected due to the process of eqn (6). The activities of ^{239}Np and ^{237}U in distilled specimens are listed in Table 3. Because the crude salt came from a strong fluorination process utilizing F_2 and the mixture salt contained 0.17 mol% UF_4, ^{239}Np and ^{237}U showed higher radioactivity before distillation. The change tendency of ^{239}Np was similar as ^{237}U, which suggested the similar volatility for ^{239}Np and ^{237}U.

$$^{238}_{92}\mathrm{U} \xrightarrow{(\mathrm{p},\ \mathrm{n})} {}^{239}_{93}\mathrm{Np} \tag{5}$$

$$^{235}_{92}\mathrm{U} \xrightarrow{(\mathrm{n},\ \gamma)} {}^{236}_{92}\mathrm{U} \xrightarrow{(\mathrm{n},\ \gamma)} {}^{237}_{92}\mathrm{U} \tag{6}$$

^{239}Np is an important nuclide in the U–Pu nuclear fuel cycle. Generally, the Purex process is used to recover neptunium in aqueous reprocessing.[24,25] In recent decades, high-temperature fluorination method has been adopted to separate U, Pu and Np.[26] Different fluorination agents and reaction temperatures were the major factors affecting the behaviours of volatile reaction products. More than 95% of ^{239}Np was found in the residual salt after distillation, which constituted the same trend found for ^{237}U.

The radioactivity change for ^{237}U agreed with the major component analysis by ICP-MS as Table 2. The content of UF_4 changed from 0.16 mol% in crude salt to 0.03 mol% in receiver salt and the relative volatility of UF_4 *vs.* LiF was 0.2. It meant UF_4 was less volatile than LiF and mainly remained in the residual salt under vacuum distillation.

The results indicated that actinide product Pa was more volatile than U and Np. It can be assumed that U and Np could be separated from the carrier salt by the volatilization method, while this was not feasible for Pa. Further studies are required to develop a continuous process that can be used for the bulk separation of real nuclear spent fuels.

Conclusions

The evaporation experiment of various nuclides from irradiated nuclear fuel was carried out using a low-pressure distillation method. The activities of radioactive nuclides were determined by an HPGe gamma spectrometer. The distillation separation process was verified, which provided data support to design process for real fuel salt treatment. Conclusions are as follows: (1) ZrF_4 and BeF_2 were more volatile than LiF, while ThF_4 and UF_4 were much less volatile than LiF, which meant ZrF_4 and BeF_2 condensed at the coolest temperature zone and ThF_4 and UF_4 remained in the residual salt. (2) Noble metal fission products, namely, molybdenum, ruthenium, and halide iodine and were hardly observed in the crude salt due to the formation and subsequent volatilization of high valent fluorides during the fluorination treatment. (3) Some salt-seeking products, such as cerium, lanthanum, barium and neodymium, were not volatile in the distillation process; decontamination factors ranged from 10 to 10^3 at different temperature zones, which indicated that it was feasible to separate alkali metal and rare earth products using distillation method. (4) For actinides, ^{239}Np showed the evaporation behaviour similar to that of ^{237}U and remained in the residual salt. Protactinium was mainly detected in the higher condensate temperature zones, and the experimental conditions affected its distribution.

Author contributions

Jinhao Zhou: writing – original draft. Junxia Geng: writing – review. Yan Luo: investigation. Rongrong Cui: data curation. Zhongqi Zhao: investigation. Haiying Fu: methodology, funding acquisition. Xiaohe Wang: radiation support. Qiang Dou: conceptualization. Wenxin Li: supervision. Jingen Chen: editing. Qingnuan Li: project administration.

Conflicts of interest

There are no conflicts to declare.

Acknowledgements

The authors thank the financial support from the National Natural Science Foundation of China (No. 21771188), the "Strategic Priority Research Program" of the Chinese Academy of Science (Grant no. XDA02030000), "Study on some key issues on Th–U Fuel cycle" (Grant no. QYZDY-SSW-JSC016). We are grateful to Free Electron Group, and appreciate their encouragement.

References

1 L. Mathieu, D. Heuer, R. Brissota, C. Garzenne, C. Le Brun, D. Lecarpentier, E. Liatard, J.-M. Loiseaux, O. Méplan, E. Merle-Lucotte, A. Nuttin, E. Walle and J. Wilson, *Prog. Nucl. Energy*, 2006, **48**, 664–679.
2 B. J. Riley, J. McFarlane, G. D. DelCul, J. D. Vienna, C. I. Contescu and C. W. Forsberg, *Nucl. Eng. Des.*, 2019, **345**, 94–109.
3 R. C. Robertson, *Conceptual Design Study Of a Single-Fluid Molten Salt Breeder Reactor*, ORNL-4541, Oak Ridge National Lab, Tennessee, 1971.

© 2021 The Author(s). Published by the Royal Society of Chemistry

Open Access Article. Published on 01 August 2021. Downloaded on 5/2/2026 3:38:09 AM.
This article is licensed under a Creative Commons Attribution-NonCommercial 3.0 Unported Licence.

4 L. X. Sun, Y. S. Niu, C. W. Hu, C. Y. Wang, Q. Dou and Q. N. Li, *J. Fluorine Chem.*, 2019, **218**, 99–104.
5 J. H. Zhou, J. L. Tan, B. Sun, Q. Dou and Q. N. Li, *Nucl. Sci. Technol.*, 2019, **30**, 102.
6 Z. H. Wang, H. Y. Fu, Y. Yang, J. X. Geng, Y. P. Jia, D. D. Huang, W. X. Li, G. Yu, Q. N. Li and Q. Dou, *J. Radioanal. Nucl. Chem.*, 2017, **311**, 637–642.
7 J. X. Geng, Y. Yang, H. Y. Fu, Y. Luo, Q. Dou and Q. N. Li, *Nucl. Sci. Technol.*, 2021, **32**, 3.
8 Y. Luo, J. X. Geng, W. X. Li, H. Y. Fu, Q. Dou and Q. N. Li, *J. Nucl. Mater.*, 2019, **525**, 48–52.
9 Z. Chen, C. F. She, H. Y. Zheng, W. Huang, T. J. Zhu, F. Jiang, Y. Gong and Q. N. Li, *J. Electrochem. Soc.*, 2018, **165**, D411–D416.
10 L. F. Tian, W. Huang, F. Jiang, H. Y. Zheng, T. J. Zhu, C. F. She, X. B. Wang, D. W. Long, Y. Gong and G. Z. Wu, *Electrochim. Acta*, 2017, **225**, 392–398.
11 H. Y. Fu, Q. Dou, Y. Yang, Z. H. Wang, J. H. Zhou and Q. N. Li, *Chinese Patent*, ZL, 201310050642.8, 2013.
12 J. R. Hightower and L. E. NcNeese, *Ind. Eng. Chem. Process Des. Dev.*, 1973, **12**, 232–236.
13 J. R. Hightower Jr and L. E. McNeese, ORNL-TM-2058, Oak Ridge National Laboratory, Tennessee, 1968.
14 H. C. Savage and J. R. Hightower, ORNL-5176, Oak Ridge National Lab, Tennessee, 1977.
15 J. W. Kigh-tower, L. E. McMeese, B. A. flannaford and H. B. Cochran, ORNL-4577, Oak Ridge National Lab, Tennessee, 1971.
16 L. X. Liu, H. W. Wang, Y. G. Ma, X. G. Cao, X. Z. Cai, J. G. Chen, G. L. Zhang, J. L. Han, G. Q. Zhang, J. F. Hu, X. H. Wang, W. J. Li, Z. Yan and H. J. Hu, *Nucl. Instrum. Methods Phys. Res., Sect. B*, 2017, **410**, 158–163.
17 Z. Q. Zhao, J. F. Hu, Z. Q. Cheng, J. X. Geng, W. X. Li, Q. Dou, J. G. Chen, Q. N. Li and X. Z. Cai, *RSC Adv.*, 2021, **11**, 7436–7441.
18 G. R. Gilmore, *Practical Gamma-Ray Spectrometry*, Wiley, Warrington, DC, 2nd edn, 2011.
19 M. A. Samad, M. I. Ali, D. Paul and S. M. A. Islam, *Jahangirnagar Univ. Environ. Bull.*, 2012, **1**, 15–24.
20 Y. Chen, D. k. Yu, L. Fu, M. Wang, D. R. Feng, Y. Z. Yang, X. M. Xue, J. F. Wang and T. C. Mu, *Phys. Chem. Chem. Phys.*, 2019, **21**, 11810–11821.
21 C. L. Yaws, *Handbook of Vapor Pressure: Volume 4: Inorganic Compounds and Elements*, Gulf publishing Company, Houston, Taxas, 1994.
22 F. J. Smith, L. M. Ferris and C. T. Thompson, ORNL-4415, Oak Ridge National Laboratory, 1969.
23 Z. Q. Cheng, X. H. Wang, Z. Q. Zhao, J. X. Geng, J. F. Hu, J. G. Chen, X. Z. Cai, W. X. Li, Q. Dou and Q. N. Li, *Radiochim. Acta*, 2021, **109**, 311–317.
24 G. Uchiyama, H. Mineo and S. Hotoku, *Prog. Nucl. Energy*, 2000, **37**, 151–156.
25 H. Y. Chen, R. J. Taylor, M. Jobson, D. A. Woodhead, C. Boxall, A. J. Masters and S. Edwards, *Solvent Extr. Ion Exch.*, 2017, **35**, 1–18.
26 J. K. Gibson and R. G. Haire, *J. Alloys Compd.*, 1992, **181**, 23–32.

© 2021 The Author(s). Published by the Royal Society of Chemistry